 CMC, vol.47, no.3, pp.203-215, 2015

Mechanical Analysis of the Coupled Gas-Solid-Thermal Model during Rock Damage

Cao Zhengzheng[1], Zhou Yuejin[1,2], Zhang Qi[1] and Wang Erqian[1]

Abstract: Gas fracturing technology is the key to the exploration for unconventional petroleum resources and other engineering industries, so the research on the coupled gas-solid-thermal model during rock damage has the important significance to the development of gas fracturing technology. By introducing rock damage variable, the coupled gas-solid-thermal model during rock damage is established in this paper, besides, the rock damage constitutive is written with MATLAB software, which is embedded in the multi-physics coupling software COMSOL in the process of numerical computation. Based on this, the damage rule of rock mass around drilling under high pressure gas is analyzed. The results show when the ratio between x direction local stress σ_x and y direction local stress σ_y is 1, the rock failure is dominated by shear damage due to the effect of gas; when the ratio between x direction local stress σ_x and y direction local stress σ_y is 1/10, pull damage appears on both sides of drilling in the direction of Y because of the effect of gas; with the passage of time, the pore pressure in the rock mass increases gradually, while the pressure gradient decreases gradually; the primary temperature of rock mass has little influence on the pore pressure.

Keywords: gas-solid-thermal model, rock damage, gas fracturing technology, damage variable.

1 Introduction

As the successful exploitation of shale gas is launched extensively in America in recent year, the shale gas resource is increasingly becoming an important supplement for conventional energy sources, which has revolutionized a new energy industry in the world [Li, Yang, Tang, Huang and Li (2006); Tong, Jing and Zimmerman (2010); Ge, Mei, Jia, Lu and Xia (2014)]. It is commonly known that the perme-

[1] State Key Laboratory for Geomechanics & Deep Underground Engineering, School of Mechanics & Civil Engineering, China University of Mining & Technology, Xuzhou 221008, China.
[2] Corresponding author: Zhou Yuejin. Tel: +86-13914884696. Email: yuejinzh@163.com

ability of shale rock is very low (less than 1mD) and most of the shale gas reservoirs need stimulation to enhance the gas productivity [Fowler and Scott (1996); Zhu and Tang (2004); Pankow, Waas and Yen (2012); Ning, Wang, Liu, Qian and Sun (2014)]. After the completion of shale gas drilling, only the drilling with natural fractures which are well developed can be put into production directly, more than 90% of the wells need to process through acidizing, fracturing and other stimulation to get the ideal output [Li, Kong and Lu (2003); Xia (2010); Wang, Zhang, Shao, Li and Zuo (2015)]. According to the experience of United States, the conventional hydraulic fracturing technology, which requires large quantities of water, can make the clay in the reservoir swelled seriously and decrease the permeability of shale rock, thereby reducing the gas productivity [Shen, Zhao and Duan (1997); Zhu, Wei, Tian, Yang and Tang (2009); Zhou, Guo, Cao and Zhang (2013)]. Besides, many shale gas formations are water-wet and under-saturated where the initial water saturation in the reservoir is less than the capillary equilibrium irreducible water saturation. The use of water-based fracturing fluids causes water to be trapped in the near-wellbore region, thereby significantly impairing the ability of gas to flow [Tang, Ma, Li and Liu (2007); Al-Ajmi and Benjeddou (2011); Cao, Zhou, Xu and Li (2014)].

In view of the weakness in hydraulic fracturing technology, the gas fracturing technology is introduced to improve the reservoir penetration to increase to shale gas production [Mahadevan, Sharma and Yortsos (2007); Xie, Gao, Ju, Fu and Zhou (2012); Xie, Xu, Wang, Guo and Liu (2014)]. The related experiment results indicate that the high pressure gas, with the characteristics of low viscosity and surface tension, will penetrate into the rock easily during the gas fracturing processes, and its threshold pressure is far smaller than that of water, especially with a high penetration rate. By introducing rock damage variable, the paper builds the coupled gas-solid-thermal mechanical model during rock damage, and the damage constitutive is written with Matlab, which is embedded in the multi-physics coupling software COMSOL in the process of numerical computation, then rock mass damage rule around drilling under high pressure gas is analyzed.

2 The coupled gas-solid-thermal model during rock damage

Since the gas seepage flow, rock deformation and heat flow process are involved in the coupled gas-solid-thermal process during rock damage, the paper establishes a gas-solid-thermal coupling mechanical model during rock damage, based on the seepage mechanics equation, the thermodynamic principle and elastic damage theory.

2.1 The control equation of rock deformation

The rock mass is simplified to be a linear elastic isotropic porous medium, then the constitutive equation of rock mass involving stress, strain, pore pressure and temperature is obtained,

$$\sigma_{ij} = 2G\varepsilon_{ij} + \frac{2G\mu}{1-2\mu}\varepsilon_{kk}\delta_{ij} - \alpha p\delta_{ij} - K\alpha_T T\delta_{ij} \tag{1}$$

In equation (1), G represents the shear modulus; μ represents Poisson's ratio; δ_{ij} represents Kronecker symbol; $\alpha = 1 - K/K_s$ represents Biot's coefficient; K represents the bulk modulus; α_T represents the thermal expansion coefficient.

According to the deformation continuity conditions, the geometric equation is shown as follows,

$$\varepsilon_{ij} = \frac{1}{2}(u_{i,j} + u_{j,i}) \tag{2}$$

Putting equation (1) and equation (2) to the equilibrium equation, the modified form of the Navier equation involving displacement, pore pressure and temperature is deduced as follows,

$$Gu_{i,jj} + \frac{G}{1-2\mu}u_{j,ji} - \alpha p_{,i} - K\alpha_T T_{,i} + f_i = 0 \tag{3}$$

2.2 The gas seepage equation

The conservation of mass is satisfied in the process of gas seepage,

$$\frac{\partial m}{\partial t} + \nabla(\rho_g q_g) = Q_m \tag{4}$$

In equation (4), m represents the gas mass per volume of rock; ρ_g represents the gas density; q_g represents the Darcy seepage velocity of the gas; Q_m represents the source origin; t represents the time variable.

The gas seepage flow in fractured medium under the drive of pressure gradient is commonly used as follows,

$$q_g = -\frac{k}{\mu_f}(\nabla p + \rho_g g\nabla z) \tag{5}$$

In equation (5), μ_f represents the dynamic viscosity coefficient; k represents the permeability of gas.

Since the gas is compressible, it could be regarded as the ideal gas, therefore the relationship between the density and pressure is obtained,

$$\rho_g = \frac{M_g p}{RT} \tag{6}$$

In equation (6), M_g represents relative molecular mass of the gas; R represents the constant value of ideal gas; T represents the absolute temperature.

Putting equation (5) and equation (6) into equation (4), the gas seepage continuity equation is deduced as follows,

$$\frac{M_g}{RT}\frac{\partial}{\partial t}(\frac{\phi p^2}{p_a}) - \frac{M_g k}{RT\mu_f}\nabla[p(\nabla p + \frac{M_g g}{RT}\nabla z)] = Q_m \tag{7}$$

The deformation of rock mass occurs under the action of gas pressure, thus changing the porosity of rock mass, and affecting the gas seepage in rock mass. The dynamic evolution model of rock porosity is obtained as follows,

$$\phi = 1 - \frac{1-\phi_0}{1+\varepsilon_v}(1 - \frac{\Delta p}{K_s}) \tag{8}$$

In equation (8), ϕ_0 represents the initial porosity; ε_v represents the volume strain; Δp represents the variation of gas pressure; K_s represents the bulk modulus of basic frame of rock mass.

According to the Kozeny-Carman equation in seepage mechanics, the permeability expression k could be obtained as follows,

$$k = \frac{k_0}{1+\varepsilon_V}(1 + \frac{\varepsilon_V}{\phi_0} - \frac{\Delta p(1-\phi_0)}{K_s\phi_0})^3 \tag{9}$$

2.3 The law of energy conservation

According to the Fourier's law, the constitutive equation of heat transfer is shown as follows,

$$q_T = -\lambda_M \nabla T + \rho_g C_g q_g T \tag{10}$$

In equation (10), q_T represents heat flow amount; $\lambda_M = (1-\phi)\lambda_s + \phi\lambda_g$, λ_s and λ_g are the heat transfer coefficient of the solid (rock mass) and the fluid (gas), respectively.

As the thermal equilibrium between rock mass and the gas is constantly kept, the heat balance equation can be expressed as follows,

$$(\rho C)_M \frac{\partial T}{\partial t} - TK_g\alpha_g\nabla\cdot(\frac{k}{\mu_f}\nabla p) + TK\alpha_T\frac{\partial \varepsilon_V}{\partial t} = -\nabla\cdot q_T \tag{11}$$

In equation (11), $(\rho C)_M$ represents the heat capacity; the first item is the variable rate of internal energy, and the second item is the heat dissipation caused by thermal expansion, and the third item is the additional item caused by deformation energy. If the internal heat source, the initial conditions and boundary conditions are given, the temperature in the rock mass in different time can be obtained.

2.4 The damage evolution equation

The tensile damage and shear damage in rock mass occur if the maximum tensile stress criterion and Mohr-Coulomb criterion is satisfied, respectively, which is shown in figure 1.

$$\begin{aligned} F_1 &= \sigma_1 - f_t = 0 \\ F_2 &= -\sigma_3 + \sigma_1((1+\sin\phi)/(1-\sin\phi)) - f_c = 0 \end{aligned} \tag{12}$$

In equation (12), σ_1 and σ_3 is the maximum principal stress and minimum principal stress, respectively; f_t and f_c is the uniaxial tensile strength and uniaxial compressive strength, respectively.

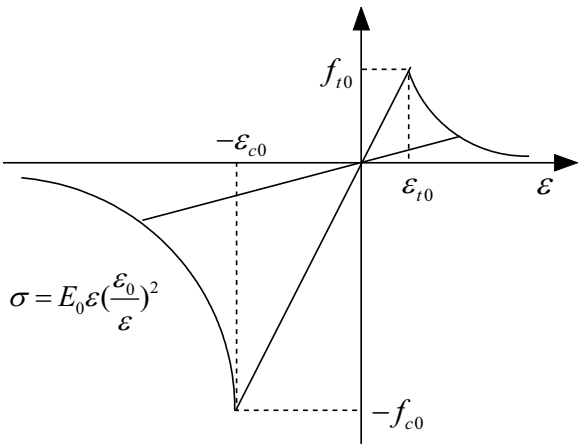

Figure 1: The constitutive law of rock under uniaxial stress condition

According to the elastic damage theory, the modulus of elasticity is shown below,

$$E = (1-D)E_0 \tag{13}$$

In equation (13), E_0 represents the modulus of elasticity before the damage occurs.

The damage variable of rock mass is shown in the following equations,

$$D=\begin{cases}0 & F_1<0, F_2<0\\ 1-\left|\dfrac{\varepsilon_t}{\varepsilon_1}\right|^2 & F_1=0, \mathrm{d}F_1>0\\ 1-\left|\dfrac{\varepsilon_c}{\varepsilon_3}\right|^2 & F_2=0, \mathrm{d}F_2>0\end{cases} \tag{14}$$

In equation (14), ε_1 and ε_3 is the maximum principal strain and minimum principal strain, respectively; ε_t and ε_c is the maximum tensile principal strain and the maximum compressible principal strain.

Due to the highly nonlinear characteristics in coupled equations, the finite element numerical method is introduced. COMSOL Multiphysics is the finite element numerical analysis software designed for multiphysical field coupling problem, and it also owns the powerful programming function based on MATLAB language or COMSOL script. In this paper, the rock damage constitutive is written with MATLAB, which is embedded in the multiphysics coupling software COMSOL in the process of numerical computation.

3 The rock damage simulation under high pressure in different in-situ stress

In order to research the rock mass damage rule under high pressure, high pressure gas is injected in drilling under the condition of initial ground stress, and then rock mass damage rule around drilling under high pressure gas is analyzed.

The numerical model is the cube 10m × 10m × 1m, whose center is the borehole (the radius 0.1 m). The elastic modulus and strength of the model unit present the rule of Weibull distribution. Assume that the initial temperature of rock mass is 55°C, and the mechanical parameters of rock mass and the coupling parameters are shown in table 1. The left and lateral boundary condition of the numerical model is the displacement constraint, while the right and upper boundary condition of the numerical model is applied external boundary stress; the pressure in the borehole increases gradually.

In order to study the influence of the gas pressure on rock mass in different in-situ stress level, two numerical models are established as follows, the stress ratio in case I is $\sigma_x/\sigma_y = 1/1$, and the stress ratio in case II is $\sigma_x/\sigma_y = 1/10$. For each case, two kinds of working condition are discussed. The first working condition is to simulate the damage zone distribution of surrounding rock in the stress ratio without the gas pressure, and external boundary stress ($\Delta\sigma_y = 1$MPa) increases according to the stress ratio (σ_x/σ_y). The second working condition is to simulate the influence of gas pressure on rock mass, and initial boundary stress ($\sigma_y = 10$MPa) increases

Table 1: Physical-mechanical parameters of rock and gas

The parameter	value
The uniaxial compressive strength s_c/MPa	60
The uniaxial tensile strength s_l/MPa	6
The initial permeability k_0/m^2	1×10^{-15}
The initial porosity ϕ_0	0.01
The dynamic viscosity coefficient μ_f/Pa·s	1.79×10^{-5}
The rock elastic modulus E/GPa	37.5
Poisson's ratio ν	0.33
The air density ρ_{ga}/Kg·m^{-3}	1.29
The heat transfer coefficient λ_s/J·(m·s·K)$^{-1}$	0.2
The rock thermal expansion coefficient α_T/K^{-1}	2.4×10^{-5}
The rock heat capacity C_s/J·(kg·K)$^{-1}$	1.25×10^3
The air heat capacity C_g/J·(kg·K)$^{-1}$	1.005×10^3

according to the stress ratio (σ_x/σ_y), and the gas pressure in the drill hole increases gradually ($\Delta p = 0.1$MPa).

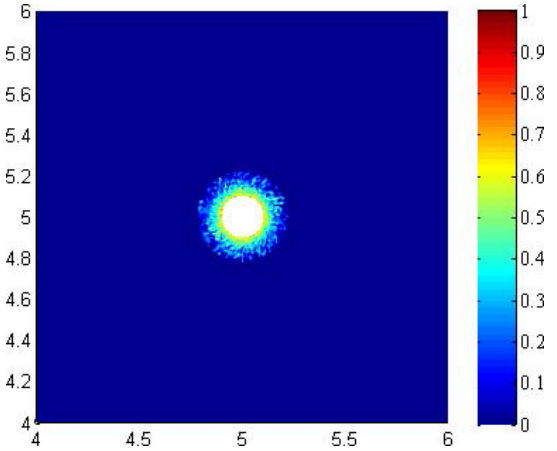

Figure 2: The distribution of damage zone without gas pressure for case I ($\sigma_y =$ 24MPa)

In order to distinguish the tensile crack and shear crack, the damage value in tensile crack is negative, while the damage value in shear crack is positive. The distribution of damage zone without gas pressure for case I ($\sigma_y = 24$MPa) is present in figure 2. A great deal of shear crack appears around the borehole rock mass under the effect

of in-situ stress, without the tensile crack. The crack and damage area increase gradually with the increase of boundary stress. The shear damage is the dominant fracture form of surrounding rock in the increase process of boundary stress, and the stress concentration appears in surrounding rock mass around the drill hole, destroying the surrounding rock mass and the overall damaged area appears.

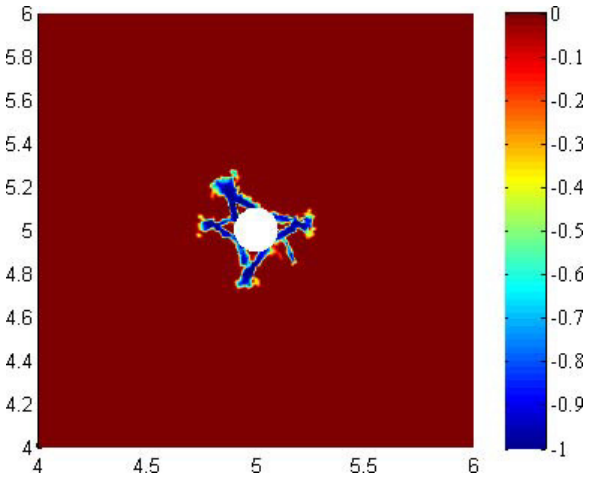

Figure 3: The distribution of damage zone with gas pressure for case I ($\sigma_y =$ 10MPa, $p =$ 7MPa)

The distribution of damage zone with gas pressure for case I ($\sigma_y =$ 10MPa, $p =$ 7MPa) is shown in figure 3. σ_y is the boundary stress in Y direction, and p is the gas pressure injected in the borehole. When the gas pressure is applied, the effective stress reaches the tensile strength of rock mass gradually with the increase of pore pressure. Tensile crack occurs in the rock mass around borehole, and it expands along with the increase of pore pressure. Compared with the figure 2, tensile damage is the dominant form in this working condition, and some tensile cracks appear. It is believed that the existence of pore pressure has the inhibitory effect on the shear damage. Since the uniaxial tensile strength of rock mass is far less than the uniaxial compressive strength, the gas pressure for rock damage is smaller.

The distribution of damage zone without gas pressure for case II ($\sigma_y =$ 22MPa) is shown in figure 4. Since the in-situ stress in X direction stress is less than that in Y direction, the tensile crack appears in the upper and down sides of drill hole due to the tensile stress, while the compression-shear crack occurs in the left and right sides under compressive stress in Y direction, and the dominant damage area appears around the drill hole.

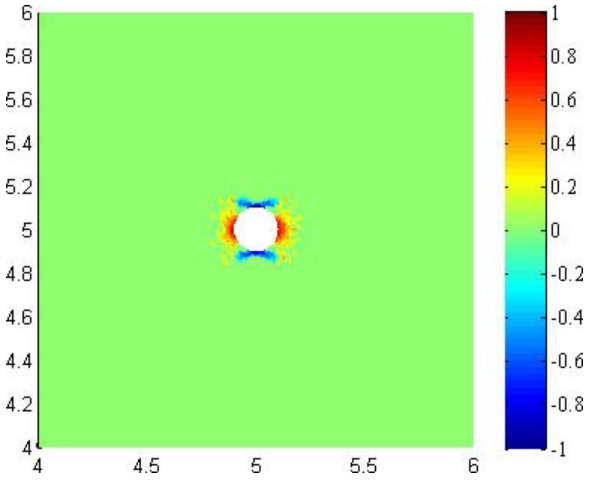

Figure 4: The distribution of damage zone without gas pressure for case II ($\sigma_y =$ 22MPa)

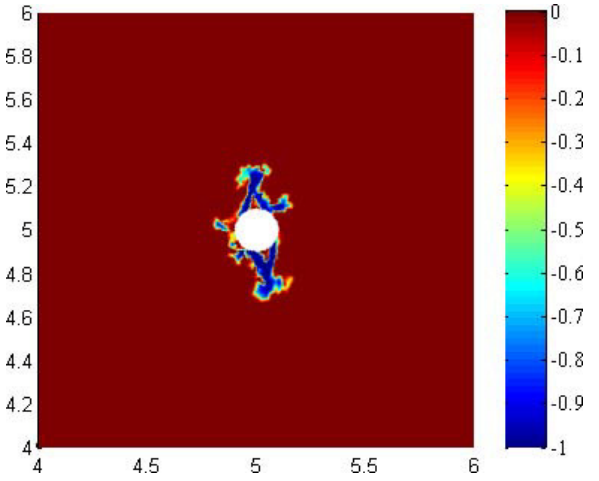

Figure 5: The distribution of damage zone with gas pressure for case II ($\sigma_y =$ 10MPa, $p = 6.2$MPa)

The distribution of damage zone with gas pressure for case II ($\sigma_y = 10$MPa, $p =$ 6.2MPa) is shown in figure 5. When the gas pressure is applied, the tensile crack occurs in upper and down sides, and expands in Y direction. Since the in-situ stress in Y direction is larger than that in X direction, the maximum principal stress in upper and down sides is greater than the maximum principal stress in left and right sides of the rock drilling. When the high pressure gas is injected in the drill hole, the rock mass in upper and down sides tends to be destroyed.

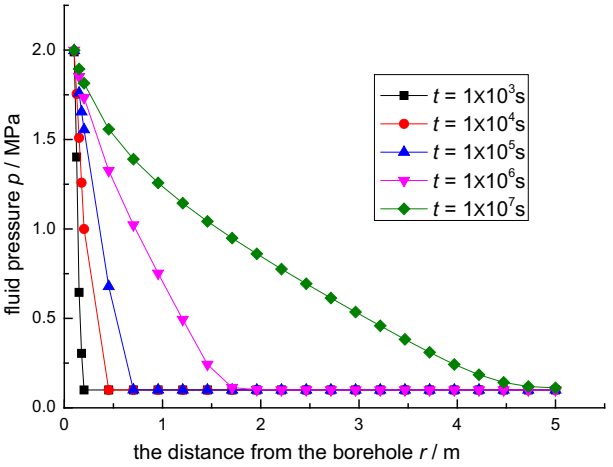

Figure 6: The distribution of fluid pressure around the borehole at different times ($T = 328$K)

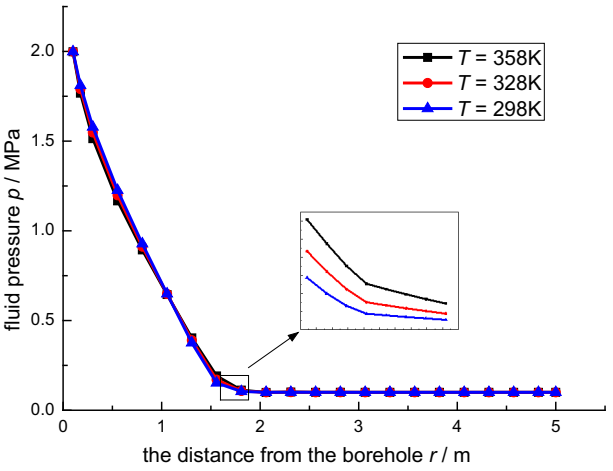

Figure 7: The distribution of temperature around the borehole under different temperature ($t = 1$e6s)

The gas (2MPa) is injected in the drill hole in different initial temperature, the pore pressure of rock mass from different distances of borehole is observed. The distribution of fluid pressure around the borehole at different times ($T = 328$K) is shown in figure 6, and the distribution of temperature around the borehole under different temperatures ($t = 1$e6s) is shown in figure 7. In figure 6, as time goes on, the pore pressure in rock mass increases gradually. The farther the distance from the borehole is, the smaller the pressure gradient is, and the pressure curve is leveling

off. In figure 7, it is believed that the change of pore pressure from the different distances of borehole with temperature is not significant in initial temperature 25°C, 55°C and 85°C. Therefore, the initial temperature of rock mass has little influence on the pore pressure.

4 Conclusions

Based on the rock mechanics, elastic mechanics and thermodynamics theory, the coupled gas-solid-thermal model during rock damage is established, and the rock damage constitutive is written with MATLAB, which is embedded in the multi-physics coupling software COMSOL in the process of numerical computation, then damage rule of rock mass around drilling under high pressure gas is analyzed. The conclusions are shown as follows,

(1) When the ratio between x direction local stress and y direction local stress is 1, the rock failure is dominated by shear damage due to the effect of gas; when the ratio between x direction local stress and y direction local stress is 1/10, pull damage appears on both sides of drilling in the direction of Y because of the effect of gas.

(2) The tensile damage is the dominant form of rock mass under high gas pressure, as the pore pressure has the inhibitory effect on the shear damage. Since the uniaxial tensile strength of rock mass is far less than the uniaxial compressive strength, the gas pressure for rock damage is smaller.

(3) As time goes on, the pore pressure in the rock increases gradually, while the pressure gradient decreases gradually. Besides, the initial temperature of rock mass has little effect on the pore pressure.

Acknowledgement: This work was supported by the Colleges and Universities in Jiangsu Province Plans to Graduate Research and Innovation (KYLX15_1407), the National Natural Science Foundation of China (51374201, 51322401, 51323004), the National Basic Research Program of China (2013CB227900), the Innovative Project of Undergraduate Student in China University of Mining and Technology (201507), the Science and Technology Major Project of Shanxi Province (2012110 1008).

References

Al-Ajmi, M.; Benjeddou, A. (2011): A new discrete-layer finite element for electromechanically coupled analyses of piezoelectric adaptive composite structures. *CMC: Computers Materials & Continua*, vol. 23, no. 3, pp. 265–285.

Cao, Z. Z.; Zhou, Y. J.; Xu, P.; Li, J. W. (2014): Mechanical response analysis and safety assessment of shallow-buried pipeline under the influence of mining. *CMES: Computer Modeling in Engineering & Sciences*, vol. 101, no. 5, pp. 351–364.

Fowler, A. C.; Scott, D. R. (1996): Hydraulic crack propagation in a porous medium. *Geophysical Journal International*, vol. 127, no. 3, pp. 595–604.

Ge, Z. L.; Mei, X. L.; Jia, Y. J.; Lu, Y. Y.; Xia, B. W. (2014): Influence radius of slotted borehole drainage by high pressure water jet. *Journal of Mining & Safety Engineering*, vol. 31, no. 4, pp. 657–664.

Li, L. C.; Yang, T. H.; Tang, C. A.; Huang, X. L.; Li, X. B. (2006): Study on coupled thermal-mechanical-damage model in rock failure process. *Rock and Soil Mechanics*, vol. 27, no. 10, pp. 1727–1732.

Li, P. C.; Kong, X. Y.; Lu, D. T. (2003): Mathematical modeling of flow insaturated porous media on account of coupling effect. *Journal of Hydrodynamics*, vol. 18, no. 4, pp. 419–426.

Mahadevan, J.; Sharma, M. M.; Yortsos, Y. C. (2007): Capillary wicking in gas wells. *SPE Journal*, vol. 12, no. 4, pp. 429–437.

Ning, J. G.; Wang, J.; Liu, X. S.; Qian, K.; Sun, B. (2014): Soft–strong supporting mechanism of gob-side entry retaining in deep coal seams threatened by rockburst. *International Journal of Mining Science and Technology*, vol. 24, no. 6, pp. 805–810.

Pankow, M.; Waas, A. M.; Yen, C. F. (2012): Modeling the response of 3D textile composites under compressive loads to predict compressive strength. *CMC: Computers Materials & Continua*, vol. 32, no. 2, pp. 81-106.

Shen, J.; Zhao, Y. S.; Duan, K. L. (1997): Numerical simulation of hydraulic fracture in low permeable coal and rock mass. *Journal of China Coal Society*, vol. 22, no. 6, pp. 580–585.

Tang, C. A.; Ma, T. H.; Li, L. C.; Liu, H. Y. (2007): Rock failure issues in geological disposal of high-level radioactive wastes under multi-field coupling function. *Chinese Journal of Rock Mechanics and Engineering*, vol. 26(Supp.2), pp. 3932–3938.

Tong, F. G.; Jing, L.; Zimmerman, R. W. (2010): A fully coupled thermo-hydro-mechanical model for simulating multiphase flow, deformation and heat transfer in buffer material and rock masses. *International Journal of Rock Mechanics and Mining Sciences*, vol. 47, no. 2, pp. 205–217.

Wang, G. G.; Zhang, J. L.; Shao, J. G.; Li, K. J.; Zuo, H.B. (2015): Investigation of non-isothermal and isothermal gasification process of coal char using different kinetic model *International Journal of Mining Science and Technology*, vol. 25, no. 1, pp. 15–21.

Xia, Y. Q. (2010): The challenges of water resources and the environmental impact of marcellus shale gas drilling. *Science & Technology Review*, no. 18, pp. 103–110.

Xie, J. L.; Xu, J. L.; Wang, F.; Guo, J. L.; Liu, D. L. (2014): Deformation effect of lateral roof roadway in close coal seams after repeated mining. *International Journal of Mining Science and Technology*, vol. 24, no. 5, pp. 597–601.

Xie, H. P.; Gao, F.; Ju, Y.; Fu, Q.; Zhou, F. B. (2012): Unconventional theories and strategies for fracturing treatments of shale gas strata. *Journal of Sichuan University (Engineering Science Edition)*, vol. 44, no. 6, pp. 1-6.

Zhou, Y. J.; Guo, H. Z.; Cao, Z. Z.; Zhang, J. G. (2013): Mechanism and control of water seepage of vertical feeding borehole for solid materials in backfilling coal mining. *International Journal of Mining Science and Technology*, vol. 23, no. 5, pp. 675-679.

Zhu, W. C.; Tang, C. A. (2004): Micromechanical model for simulating the fracture process of rock. *Rock Mechanics and Rock Engineering*, vol. 37, no. 1, pp. 25-56.

Zhu, W. C.; Wei, C. H.; Tian, J.; Yang, T. H.; Tang, C. A. (2009): Coupled thermal-hydraulic-mechanical model during rock damage and its preliminary application. *Rock and Soil Mechanics*, vol. 30, no. 12, pp. 3851–3857.